arXiv:nlin/0010038v1 [nlin.CD] 23 Oct 2000

Quantum correlations and classical resonances in an open chaotic system

Wentao T. Lu, Kristi Pance, Prabhakar Pradhan and S. Sridhar*
Physics Department, Northeastern University, Boston, Massachusetts 02115.

February 8, 2008

Abstract

We show that the autocorrelation of quantum spectra of an open chaotic system is well described by the classical Ruelle-Pollicott resonances of the associated chaotic strange repeller. This correspondence is demonstrated utilizing microwave experiments on 2-D n-disk billiard geometries, by determination of the wave-vector autocorrelation $C(\kappa)$ from the experimental quantum spectra $S_{21}(k)$. The correspondence is also established via "numerical experiments" that simulate $S_{21}(k)$ and $C(\kappa)$ using periodic orbit calculations of the quantum and classical resonances. Semiclassical arguments that relate quantum and classical correlation functions in terms of fluctuations of the density of states and correlations of particle density are also examined and support the experimental results. The results establish a correspondence between quantum spectral correlations and classical decay modes in an open systems.

Pacs ref: 05.45.Mt, 05.45.Ac, 03.65.Sq, 84.40.-x

1 Introduction

The correspondence between quantum and classical mechanics has turned out to be particularly rich for systems that are classically chaotic [1]. This correspondence is usually considered in terms of the asymptotic behavior of quantum properties. Statistical analysis of the quantum spectra of closed chaotic systems display short-range correlations that are universal and can be described by random matrix theory (RMT) [2, 3]. The long range behavior of spectral fluctuations require semiclassical treatments that incorporate periodic orbits[4].

In this paper we establish a new connection between the statistics of quantum spectra and classical dynamical properties of an open chaotic system, utilizing physical and numerical experiments on the well-known n-disk billiard geometry. The n-disk system [5] is a paradigm of open hyperbolic systems, with an associated strange repeller [6] whose strange properties arise from the Cantor set of the unstable periodic orbits (PO). For hyperbolic repellers, Ruelle [7] and Pollicott [8] showed that the dynamical evolution of repellers toward equilibrium can be expressed in terms of complex poles, leading to the so-called Ruelle-Pollicott (RP) resonances. The n-disk billiards have been extensively addressed theoretically, both classically and semiclassically [5, 9, 10, 11], and only recently have been studied experimentally [12, 13].

Our microwave experiments on the n-disk billiards measure the quantum transmission spectrum $S_{21}(k)$, which is essentially the two-point Green's function $G(\vec{r}_1, \vec{r}_2, k)$, and from which the spectral autocorrelation $C(\kappa)$ is determined. The small wave vector κ (long time) behavior of the spectral autocorrelation provides a measure of the quantum escape rate, and is in good agreement with the corresponding classical escape rate γ_{cl} [12, 13], as predicted by RMT analysis of this universal behavior. For large $\kappa > \gamma_{cl}$ (short time), non-universal oscillations of the autocorrelation $C(\kappa)$ are observed, that can be understood completely in terms of classical RP resonances. This behavior is similar to that of the variance $\Sigma^2(L)$ of closed chaotic systems, which also displays leading universal behavior for small L, followed by non-universal behavior for large L that can be described in terms of system specific periodic orbits [4]. The present work demonstrates that $C(\kappa)$ of open systems displays a similar trend from short-range universality to long-range non-universality, however the non-universal contributions to quantum correlations are described in terms of other classical phase space structures of the associated repeller, viz. the RP resonances [14].

A concise account of the main results was presented in Ref. [15]. This paper further explores the details of the experimental aspects, as well as confirming the results via numerical experiments using simulated quantum spectra. Semiclassical arguments that demonstrate this correspondence are discussed in terms of fluctuations of the density of states and correlations of the particle density. The wider implications of the present results are also discussed.

2 Experimental results

The quantum dynamics of the 2-D n-disk system can be realized in a microwave experiment exploiting the mapping between the Helmholtz equation and the Schrödinger equation in their stationary forms and in the 2-D limit. This is because under the conditions of the experiment, the Maxwell-Helmholtz equations reduce to

---

*e-mail: srinivas@neu.edu

$(\nabla^2 + k^2)\Psi = 0$ with $\Psi = E_z$ the microwave electric field. The experimental geometry consists of thin copper disks sandwiched between two large copper plates of size 55×55 cm^2 in area. In order to simulate an infinite system, microwave absorber material ECCOSORB AN-77 was placed between the plates at the edges. Microwaves were coupled in and out through antennas inserted in the vicinity of the scatterers. All measurements were carried out using an HP8510B vector network analyzer which measured the complex transmission amplitude (S_{21}) and reflection amplitude (S_{11}) S-parameters of the coax + scatterer system. An example of the measured transmission $T(k) = |S_{21}(k)|^2$ of a 4-disk system is shown in Fig. 1. For more details of the microwave experiments, see Ref. [13].

An open system can be represented by an effective Hamiltonian consisting of two parts, $H = H_c + iW$, where H_c is the Hamiltonian for the closed system and $W = W^\dagger$ represents the decay to open channels. Since the total Hamiltonian is not Hermitian, the eigenfunctions ψ_n of H with eigenvalues E_n do not form an orthogonal set. Instead, let ϕ_n be the eigenfunction of the adjoint operator $H^\dagger$ with eigenvalues E_n^*, and the ψ's and ϕ's form a bi-orthonormal set with $\int \psi_m^*(\vec{r})\phi_n(\vec{r})d\vec{r} = \delta_{mn}$. The Green's function for an open system is [16] $G(\vec{r}_1, \vec{r}_2, k) = \sum_n \frac{\psi_n^*(\vec{r}_1)\phi_n(\vec{r}_2)}{E - E_n}$. For the n-disk system, with the quantum resonances in wave vector space $k_n = s_n + is'_n$, we have

$$|G(\vec{r}_1, \vec{r}_2, k)|^2 = \frac{2m}{\hbar^2}\sum_n \frac{|\psi_n(\vec{r}_1)\phi_n(\vec{r}_2)|^2}{[(k+s_n)^2 + s_n'^2][(k-s_n)^2 + s_n'^2]} + \frac{2m}{\hbar^2}{\sum_{n,m}}' \frac{\psi_n^*(\vec{r}_1)\phi_n(\vec{r}_2)\psi_m(\vec{r}_1)\phi_m^*(\vec{r}_2)}{(k^2 - k_n^2)(k^2 - k_m^2)^*}.$$

The second sum with the prime includes the off-diagonal terms with $n \neq m$. Their contribution can be neglected if all the resonances are well separated.

The transmission amplitude $S_{21}(k)$ measured between two point antennas is essentially the Green's function $G(\vec{r}_1, \vec{r}_2, k)$ of the system, so that $S_{21}(k) = A(k)G(\vec{r}_1, \vec{r}_2, k)$ with $A(k)$ a slowly-varying modulating function [13]. Setting $c_n = (2m/\hbar^2)|A(k)\psi_n(\vec{r}_1)\phi_n(\vec{r}_2)|^2/[(k+s_n)^2 + s_n'^2]$, and ignoring the off-diagonal terms, we get the transmission coefficient $T(k)$ expressed as a sum of Lorentzian peaks

$$T(k) \simeq \sum_n \frac{c_n}{(k-s_n)^2 + s_n'^2}. \tag{1}$$

The coupling c_n in Eq. (1) depend on the location of the probes. The k dependence of c_n is locally weak near a resonance since $1/[(k+s_n)^2 + s_n'^2]$ is flat around $k \sim s_n \gg s'_n$ for sharp resonances. One can treat c_n practically as constants in the neighborhood of a resonance. This shows that the measured transmission coefficient $T(k)$ shown in Fig. 1 directly yields the wave-vector s_n and the half-width s'_n of the sharper scattering resonances. We next compare the experimental resonances with semiclassical calculations.

2.1 Calculation of Quantum Resonances

Although any chaotic system can be quantized numerically by directly diagonalizing the Hamiltonian truncated in certain expansion space, for a large number of systems, one uses the techniques based upon semiclassical periodic orbit theory [1], such as the cycle expansion [17], Fredholm determinant [18] or harmonic inversion [19]. Except for the lowest eigenvalues, the semiclassical quantization gives very accurate results. Using Gutzwiller's trace formula [1], the semiclassical Ruelle zeta-function can be derived as an *Euler* product over all the prime PO which are the PO without repetition [10, 11]

$$\zeta_{j,sc} = \prod_p (1 - t_{p,sc})^{-1}, \tag{2}$$

with $t_{p,sc}$ the semiclassical weight

$$t_{p,sc} = (-1)^{l_p}\exp(ikL_p)/|\Lambda_p|^{1/2}\Lambda_p^j. \tag{3}$$

Here l_p is the number of collisions of the PO with the disks, L_p is the length of the PO and Λ_p the eigenvalue of the instability matrix $\mathbf{J}_p$. j comes in from the decomposition of the trace of the Green's function into Ruelle zeta-functions with $j = 0, 1, \cdots$. The quantum resonances are the poles of the Ruelle zeta-functions which is directly related to the trace of scattering matrix or the trace of the Green's function. If a symbolic dynamics exists for the system, only a few prime POs will be needed in the zeta-function to give quite accurate eigenvalues because the curvature in the cycle expansion will decay exponentially with increasing PO length [17].

As an example, consider the non-chaotic 2-disk system with disk separation R and disk radius a. There is only one unstable prime PO between the disks. The symmetry group of PO is C_2, with two one-dimensional irreducible representations, symmetric A_1 and anti-symmetric A_2. The semiclassical resonances in wave vector space are $k_n = [n\pi + i(1/2)\ln\Lambda]/(R - 2a)$ with $\Lambda = \sigma - 1 + \sqrt{\sigma(\sigma - 2)}$ the eigenvalue of the instability matrix in the fundamental domain and $\sigma = R/a$. Here n is odd for A_1 representation, n even and $n \neq 0$ for A_2 representation [20].

For the chaotic n-disk system with $n \geq 3$, there is no analytical expression of the semiclassical quantum resonances. To do the numerical calculations of the quantum resonances, use can be made of the symmetry of the system and the cycle expansion in the fundamental domain [10, 11]. We have calculated numerically the quantum resonances of the 3-disk and 4-disk systems with different disk separation ratio σ by searching the poles of the Ruelle zeta function (2). An example of the results of the calculation for the s_n, s'_n for a 3-disk system is shown in Fig. 2. The experiments only access a small range of the quantum resonances with $0 < \mathrm{Re}(f) < 20GHz$ and $-0.3GHz < \mathrm{Im}(f) < 0$. The experimental quantum resonances are well matched by the sharp resonances from the semiclassical calculations. The very broad resonances are not observed because the coupling to them is weak. For details concerning the comparison of experimental and calculated quantum resonances, see Ref. [13].

2.2 Experimental Spectral Autocorrelation $C(\kappa)$

The spectral autocorrelation function is determined from the experimental spectra as $C_T(\kappa) = \langle T(k-(\kappa/2))T(k+(\kappa/2))\rangle_k$ with average carried out over a band of wave vector centered at certain value k_0 and of width Δk [13]. The spectral autocorrelation can be fitted well by a superposition of Lorentzians :

$$C_T(\kappa) = \sum_{\pm,n=1}^{\infty} \frac{b_n \gamma'_n}{\gamma'^2_n + (\kappa \pm \gamma''_n)^2}, \tag{4}$$

with $\gamma'_n \pm i\gamma''_n$ the classical RP resonances in wave vector space. A semiclassical derivation will be given in Sec. 3.

The experimental RP resonances are obtained by fitting the experimental autocorrelation as shown in Fig. 3 with Eq. (4). Similar comparisons between experiment and theory for the n-disk system with $n = 2, 3, 4$ are presented in Ref. [15]. The coupling b_n in the above equation which should depend on the location of the probes determine the decay probability of the classical RP resonances. Since we do not have knowledge of them experimentally, they are chosen to optimize the fitting.

The experimental RP resonances (γ'_n, γ''_n) obtained from the Lorentzian decomposition of the experimental $C(\kappa)$ as shown in Fig. 3 are displayed in Table 1. They can be compared with theoretically calculated RP resonances, which are the poles of the classical Ruelle zeta-function, and whose calculation will be explained in the next subsection. Although the position of the peaks of the oscillations in the experimental autocorrelation in Fig. 3 is quite accurately given by the imaginary part γ''_n of the RP resonances, the experimental half-width of the oscillation is almost always smaller than the calculated real part γ'_n of the RP resonances. This is possibly because the absorber used is not ideal, and leads to quantum resonances that are slightly sharper than calculated. This results in systematically sharper widths of the experimental RP resonances.

2.3 Calculation of Classical resonances

The theoretical RP resonances are essential ingredients of a Liouvillian description of the classical dynamics, and can be calculated as the poles of the classical Ruelle zeta-function. The classical dynamics of Hamiltonian flow in symplectic phase space can be described by the action of a linear evolution operator which is also the Perron-Frobenius operator $\mathcal{L}^t(y,x) = \delta(y - f^t(x))$. Here $f^t(x)$ is the trajectory of the initial point x in phase space. The trace of the Perron-Frobenius operator is $\mathrm{tr}\mathcal{L}^t = \int \delta(x - f^t(x))dx = \sum_p T_p \sum_{r=1}^{\infty} \delta(t - rT_p) \left|\det(\mathbf{1} - \mathbf{J}_p^r)\right|^{-1}$. The first summation is over all the prime classical PO p with period T_p, the second one is over the repetition r of the prime PO. $\mathbf{J}_p$ again is the instability matrix. The evolution operator has a Lie group structure $\mathcal{L}^t = e^{-At}$ with A the generator of the Hamiltonian flow. This generator A has the classical resonances as its eigenvalues, $\gamma_n = \gamma'_n \pm i\gamma''_n$, which we call the RP resonances [7, 8]. We have $\mathrm{tr}\mathcal{L}^t = \sum_{n=0}^{\infty} g_n e^{-\gamma_n t}$, with g_n the multiplicity of the resonances. These resonances determine the time evolution of any classical quantity. The trace formula for classical flows is obtained from the Laplace transform of the above expression [21]

$$\begin{aligned} \mathrm{tr}\mathcal{L}(s) &= \int_0^{\infty} dt e^{st} \mathrm{tr}\mathcal{L}^t = \mathrm{tr}(A - s\mathbf{1})^{-1} \\ &= \sum_p T_p \sum_{r=1}^{\infty} \frac{e^{rsT_p}}{\left|\det(\mathbf{1} - \mathbf{J}_p^r)\right|}. \end{aligned} \tag{5}$$

In order to calculate the RP resonances, the Ruelle zeta-function is introduced as

$$\zeta_{\beta,cl} = \prod_p (1 - t_{p,cl})^{-1}. \tag{6}$$

Here the product is over all the prime PO with $t_{p,cl}$ the classical weights of the periodic orbits

$$t_{p,cl} = \exp(sT_p)/|\Lambda_p|\Lambda_p^{\beta-1}. \tag{7}$$

Here the integer $\beta > 0$ comes in from the expansion of the determinant $\left|\det(\mathbf{1} - \mathbf{J}_p^r)\right|^{-1}$. One can see that the above classical Ruelle zeta-function is very similar to the semiclassical one (Eq.(2)). The classical Ruelle zeta-function is exact and can be directly derived from the above trace formula (5) of the Perron-Frobenius operator. The topological pressure $P(\beta)$ can be defined as the simple pole of the classical Ruelle zeta-function [22] with β extrapolated to the entire real space. All the characteristic quantities of the classical dynamics, such as the Kolmogorov-Sinai entropy, escape rate, fractal dimensions, can be derived from $P(\beta)$ [9]. For the hard-disk system, the classical velocity v of particles is constant. So $T_p = L_p/v$. For simplicity, one can set $v = 1$. The RP resonances are then calculated in wave-vector space.

For example, the classical RP resonances of the 2-disk system are $\gamma_n = [\ln \Lambda + in\pi]/(R-2a)$ with Λ given before. Here n is even for A_1 representation and n odd for A_2 representation. Similar to the situation of the quantum resonances $s_n + is'_n$, there is no analytical expression of the RP resonances $\gamma'_n \pm i\gamma''_n$ for the chaotic n-disk system. They can be calculated numerically as the poles of the classical Ruelle zeta-function Eq. (6) [9]. 14 prime PO up to period 3 were used in our calculation of the RP resonances of the 4-disk system, the results of which are shown in Table 1.

2.4 Numerical simulation

To gain further insight into the established experimental correspondence, we have utilized the results of the calculations of the quantum and classical resonances to carry out a numerical simulation of the physical experiment. We calculate numerically a close approximation to the experimental quantum spectrum using the quantum resonances. We them determine the spectral autocorrelation of the simulated spectrum, and compare its decomposition with the calculated classical resonances.

Writing Eq. (1) explicitly, we have following form of the transmission $T(k) \simeq (2m/\hbar^2)|A(k)|^2 \sum_n \frac{|\psi_n(\vec{r}_1)\phi_n(\vec{r}_2)|^2}{[(k+s_n)^2+s'^2_n][(k-s_n)^2+s'^2_n]}$. Here we assume the presence of the probes poses a small perturbation and will not change the quantum spectrum. For a closed chaotic system with time-reversal symmetry, the wave density is expected to follow the Porter-Thomas (PT) distribution in RMT [23]. For a very open system and when the probes are far away from the scatterers, the wave density will not follow the PT distribution. But in the vicinity of the scatterers, one may assume the density to follow the PT distribution. Setting $\rho_{1n} = |\psi_n(\vec{r}_1)|^2$ and $\rho_{2n} = |\phi_n(\vec{r}_2)|^2$, one has, $P(\rho_n) = (2\pi\rho_n\overline{\rho})^{-1/2}\exp(-\rho_n/2\overline{\rho})$ with $\overline{\rho}$ being the ensemble averaged density. The densities at the location of different antennas were found not to be correlated in closed cavities [24]. We assume the same is true for an open chaotic system in the vicinity of the scatterer disks. For simplicity, we consider the ensemble average of the transmission coefficient $\overline{T(k)} \simeq (2m/\hbar^2)|A(k)|^2\overline{\rho}_1\overline{\rho}_2\sum_n 1/\left[(k+s_n)^2+s'^2_n\right]\left[(k-s_n)^2+s'^2_n\right]$. From this expression, one can see that the contribution from broad resonances is suppressed. The main contribution is from sharp resonances. This has already been observed in our experiments[12, 13]. For these sharp resonances, if they are far away from the origin, $(k+s_n)^2+s'^2_n \simeq 4k^2$. Thus, for large $k \gg s'_n$, the above transmission can be approximated as $\overline{T(k)} \simeq (2m/\hbar^2)|A(k)|^2(\overline{\rho}_1\overline{\rho}_2/4k^2)\sum_n\left[(k-s_n)^2+s'^2_n\right]^{-1}$. The function $A(k)$ is found to be proportional to k [25, 26]. For convenience, we set $A(k) = 2k$ and also $(2m/\hbar^2)\overline{\rho}_{1n}\overline{\rho}_{2n} = 1$. We thus get

$$\overline{T(k)} \simeq \sum_n \frac{1}{[(k-s_n)^2+s'^2_n]}. \tag{8}$$

The k dependence of $A(k)$ can be understand as follows. In the experimental setup, one of the antenna can be regarded as a diploe radiating electromagnetic waves. The radiated electrical field of a dipole is proportional to k if an alternating current with constant amplitude I_{in} was maintained on it [27]. The voltage picked up on another antenna is just the electrical field at the antenna location times the length d of the antenna inside the cavity. The transmission amplitude S_{21} measured by the analyzier is the ratio of the output voltage on one antenna to the input current of another antenna, $S_{21} = dE_{z,\text{out}}/I_{\text{in}}$, thus $A(k) = dE_{z,\text{in}}/I_{\text{in}} \propto k$.

The expression (8) is thus used to get the averaged transmission and then to calculate the autocorrelation $C_T(\kappa)$ numerically. We have done that for the n-disk system with $n = 2, 3, 4$ using $a = 5$cm. Here we just present the results for the 3-disk system as shown in Fig. 4 and 5. Note that $f = (c/2\pi)k$, $1GHz$ is equivalent to 0.2096cm^{-1}. The symmetry group for the chaotic 3-disk system is C_{3v} [10], which has two one-dimensional irreducible representations A_1, A_2, and one two-dimensional irreducible representation E. In the fundamental domain, only the resonances of the A_2 representation will contribute to the transmission [12]. The semiclassical resonances of A_2 representation in the range $0 < \text{Re}\,ka < 100$ and $-0.5 < \text{Im}\,ka < 0$ for the disk separation $R/a = 4\sqrt{3}$ are obtained from $\zeta_{sc}(ik)$ with $j = 0$. About 200 resonances are obtained as shown in Fig. 2.

The corresponding classical resonances shown in Fig. 5 are from the A_1 representation of the classical Ruelle zeta-function (6) with $\beta = 1$. 8 prime PO up to period 4 were used in our calculations of the quantum and RP resonances. The numerical transmission and the autocorrelation are shown in Fig. 4 and 5, respectively. One can see that the oscillations in the autocorrelation are fully determined by the classical RP resonances as predicted by Eq.(4).

3 Quantum and classical correlations

In the above section, we have demonstrated experimentally and numerically that the quantum auto-correlation and hence the statistics of quantum resonances are determined by the RP resonances of the underlying classical dynamics. Here we explore the theoretical justification for this correspondence.

For chaotic open scattering systems, the distribution and correlation of the quantum resonances have been discussed in the framework of RMT [28]. However, the RMT results are the ensemble averages of different systems with certain symmetry in common. Consequently, RMT does not make contact with system specific features of the underlying classical dynamics. Thus it is unable to make any concrete connection between the quantum and classical dynamics, for which it is necessary to go beyond RMT.

The appearance of nonuniversality requires the use of structures such as periodic orbits within semiclassical calculations. To proceed, we first consider the correlation of the density of states. In the semiclassical periodic orbit theory, the fluctuation part of the density of states is [1]

$$\begin{aligned}\mathcal{D}(k) &= -\frac{1}{\pi}\,\mathrm{Im}\,\mathrm{tr}G(\vec{r}_1,\vec{r}_2,k) \\ &= -\frac{1}{\pi}\,\mathrm{Im}\sum_p T_p \sum_{r=1}^{\infty} \frac{e^{irkL_p}}{\left|\det(\mathbf{1}-\mathbf{J}_p^r)\right|^{1/2}}. \qquad (9)\end{aligned}$$

The trace of the Green's function is the integration over the configuration space with $\vec{r}_1 = \vec{r}_2$. The autocorrelation is

$$C_{\mathcal{D}}(\kappa) = \frac{1}{2K}\int_{-K}^{K} dk\mathcal{D}(k+\frac{\kappa}{2})\mathcal{D}(k-\frac{\kappa}{2}), \quad K \gg \kappa.$$

Substituting the semiclassical expression (9) of $\mathcal{D}(k)$ into the above equation, one gets [29]

$$\begin{aligned}C_{\mathcal{D}}(\kappa) &= \mathrm{Re}\sum_p T_p^2 \sum_{r=1}^{\infty} \frac{e^{rsT_p}}{\left|\det(\mathbf{1}-\mathbf{J}_p^r)\right|} \simeq \mathrm{Re}\,\mathrm{tr}\frac{1}{A-s\mathbf{1}} \\ &= \sum_n \frac{1}{\upsilon}\left[\frac{\gamma_n'}{\gamma_n'^2+(\kappa+\gamma_n'')^2} + \frac{\gamma_n'}{\gamma_n'^2+(\kappa-\gamma_n'')^2}\right] \qquad (10)\end{aligned}$$

with $s = i\upsilon\kappa$. Since the spectrum of the generator A is $\upsilon(\gamma_n' \pm i\gamma_n'')$, one can see that in the semiclassical theory, the autocorrelation of the density of states is determined solely by the classical RP resonances. The transmission spectrum $T(k)$ is a projection of the density of states, one expects that the autocorrelation of the transmission is also determined by the RP resonances. The approximation in Eq. (10) is valid only for hyperbolic systems with finite symbolic dynamics. For these systems as explained in Sec. 2.1, the contribution to the autocorrelation $C_{\mathcal{D}}(\kappa)$ is mainly from a few fundamental prime POs. For those PO, one has $T_p^2 \simeq \overline{T}T_p$ with $\overline{T}$ the average period. For weakly open or closed system, the approximation will break down.

The experimental quantity whose correlations we examined in Sec. 2 is the Green's function, while theoretical arguments usually examine the density of states or the time delay [30] which are however not directly measurable experimentally. To develop the correlation theory for the transmission we measured, consider the stationary Green's function $G(\vec{r},\vec{r}_0,k)$ which is the solution of the following equation $(\nabla^2+k^2)G(\vec{r},\vec{r}_0,k) = \delta(\vec{r}-\vec{r}_0)$, with certain boundary condition. The quantum mechanical propagator is the Fourier transform of the Green's function. One can construct a time evolution of a wave packet $\hat{K}(\vec{r},\vec{r}_0,t)$ with $\hat{K}(\vec{r},\vec{r}_0,t) = (2\pi\hbar i)^{-1}\int_{\Delta\varepsilon} G(\vec{r},\vec{r}_0,\sqrt{2m\varepsilon/\hbar^2})e^{-i\varepsilon t/\hbar}d\varepsilon$, with $\varepsilon = \hbar^2k^2/2m$. Here the integration is performed around $\varepsilon_0 = \hbar^2k_0^2/2m$, with the range $\Delta\varepsilon = \hbar\upsilon\Delta k$ and $\upsilon = \hbar k_0/m$ the group velocity of the wave packet. The integration in the ε space can be changed into that in the k space. We get $\hat{K}(\vec{r},\vec{r}_0,t) = e^{-i\varepsilon_0 t/\hbar}(\upsilon/2\pi i)\int_{\Delta k} G(\vec{r},\vec{r}_0,k_0+k)e^{-i\upsilon kt}dk$. The propagator $\hat{K}(\vec{r},\vec{r}_0,t)$ is just the wave function at point $\vec{r}$ due to a δ-function excitation of the system at point $\vec{r}_0$ and time $t_0 = 0$. The particle density $\rho(t)$ is thus

$$\begin{aligned}\rho(t) = \left|\hat{K}(\vec{r},\vec{r}_0,t)\right|^2 &= \frac{\upsilon^2}{4\pi^2}\int_{\Delta k} G(\vec{r},\vec{r}_0,k_0+k)e^{-i\upsilon kt}dk \\ &\times \int_{\Delta k} G^*(\vec{r},\vec{r}_0,k_0+k')e^{i\upsilon k't}dk',\end{aligned}$$

with the average given by $\langle\rho(t)\rangle_t = \lim_{T\to\infty} T^{-1}\int_0^T \rho(t)dt = (\upsilon^2/2\pi L)\int dk\,|G(k)|^2$. A probability measure is assumed for the above average to converge [7]. Here L is the size of the whole system. For an open system, $L \to \infty$. Here we used the definition of the δ function $\delta(t) = (2\pi)^{-1}\int d\omega e^{-i\omega t}$.

The autocorrelation of the particle density is

$$C_\rho(\tau) = \langle\rho(t)\rho(t+\tau)\rangle_t - \langle\rho\rangle_t^2.$$

Using the diagonal approximation, we get

$$C_\rho(\tau) = \frac{\upsilon^4\Delta k}{4\pi^2L^2}\int d\kappa C_T(\kappa)e^{-i\upsilon\kappa\tau}. \qquad (11)$$

Note that we have $T(k) \propto |G(\vec{r},\vec{r}_0,k)|^2$.

If one assumes that the correlation of the particle density is classical, one has [31]

$$C_\rho(\tau) = \sum_{n=0}^{\infty} 2b_n' e^{-\gamma_n'\upsilon\tau}\cos\gamma_n''\upsilon\tau, \qquad (12)$$

where the coefficients b_n' are the coupling, and $\gamma_n' \pm i\gamma_n''$ the RP resonances evaluated in wave-vector space. The Fourier transformation of (11) and (12) gives

$$C_T(\kappa) = \sum_{\pm,n=0}^{\infty} \frac{b_n\gamma_n'}{\gamma_n'^2+(\kappa\pm\gamma_n'')^2}. \qquad (13)$$

with $b_n = 2\pi L^2 b_n'/\upsilon^4\Delta k$. The autocorrelation is usually normalized as $C_T(0) = 1$ so that the system size L will be cancelled. Thus the above expression is valid for both closed and open systems.

The above arguments closely parallel Agam's [32] recent application of the diagrammatic techniques for disordered systems to open chaotic systems. We remark that the above arguments differ somewhat from those of Agam, whose results are valid when the two probes are far away from each other which implies $\langle T^2 \rangle = 2 \langle T \rangle^2$. This is the case in the diffusive limit with a Poisson distribution of the transmission coefficient T.

The above correspondence between the autocorrelation derived from semiclassical theory and the classical resonances is obviously not exact, but requires corrections due to quantum interference. These corrections are small for open systems, but are expected to dominate for closed systems.

4 Discussion and concluding remarks

The results presented here establish an alternative path from quantum to classical achieved by considering the correspondence of quantum correlations and classical decay modes. As Fig. 3 shows, the small κ behavior of $C(\kappa)$ is universal, while the large κ behavior shows nonuniversal oscillations that are completely described by the classical RP resonances. This demonstrates that in an open system, quantum correlation functions are intimately related to decay laws of classical survival probabilities or evolution of particle ensembles.

Most theoretical calculations in quantum chaos using ensemble averaging are restricted only to the leading order consistent with RMT, which probes only the average properties of the system, such as the average escape rate γ. The leading RMT contribution to the correlation $C(\kappa)$ is Lorentzian [33, 34, 35, 36, 12] $C(\kappa) = C(0)/(1 + (\kappa/\gamma_{cl})^2)$, when the classical decay is exponential, which occurs for hyperbolic systems such as the n-disk billiards. Our earlier experiments established this result in the open microwave billiards [12].

As we have shown, our experiments go well beyond the average information represented by RMT - the spectral data contain further details of the fine structure embodied in the decay modes or classical resonances of the system. In terms of the fractal repeller, the wave mechanical experiments thus yield not only the leading average property γ_{cl} related to the fractal dimension, but also further higher order properties of the repeller in terms of the classical resonances. While we have demonstrated this for the n-disk billiard, the above result should be valid generally for hyperbolic open chaotic systems.

The relevant classical limit here is the evolution of classical particle ensembles. The notion of ensemble averaging that is common in quantum mechanics is also useful in classical treatments of chaotic systems. This is because while the prediction of individual particles is sensitive to initial conditions, the dynamics of appropriate averages of a perturbed system relaxing towards equilibrium is well defined. The RP resonances determine the decay modes of the dynamical systems evolving from a nonequilibrium state to equilibrium or steady state. For an open system, Gaspard and Nicolis [39] have derived an escape rate formula to relate the coefficient of diffusion and the escape rate of large open systems. While for an open system, the escape rate γ_0 is nonvanishing, for closed system, $\gamma_0 = 0$, and the corresponding eigenstate is just the equilibrium state. The RP resonances are essential ingredients of a description of irreversibility and thermodynamics based upon microscopic chaos [40, 9, 41]. However these resonances have remained mathematical objects. The present experiments have provided physical reality to them. It is remarkable that we are able to observe classical resonances in a quantum experiment. Because microwaves do not interact (collide) with each other, ensemble averaging is easier to achieve in microwaves than in fluids. Thus theories that employ ensemble averaging are ideally applicable to the microwave experiments. This is true for both open systems as shown here, and for disordered billiards [42].

The present work shows that the information concerning the classical resonances is coded into the quantum spectrum. This is somewhat anticipated in periodic orbit theory, where one can observe the strong similarity between the classical (Eq.(6) and (7)) and semiclassical (Eq.(2) and (3)) Ruelle zeta-functions. A one-to-one correspondence exists between k_n and γ_n for the 2-disk system as discussed in Sec.I. Another example where an exact relation between the classical and quantum resonances exists is the system of a free particle sliding on a compact surface of constant negative curvature, the RP resonances were found by Biswas and Sinha [37] to be $\gamma_0 = 0$, $\gamma_n = \frac{1}{2} \pm ip_n$ for $n \geq 1$ with real p_n the solution of a certain equation while the quantal excitation eigenvalues are $E_n = p_n^2 + \frac{1}{4}$. One would also expect a relation between the distribution of the classical and semiclassical resonances. The RP resonances have recently been observed in the distribution of the zeroes of the Riemann zeta function [38].

Our work demonstrates that suitable quantum correlations diffuse just like classical observables in an open system. An interesting question is what will happen when the number n of disks are very large, a situation that is frequently referred to as the Lorentz gas. Due to the exponential separation of the nearby orbits, a particle is forced to move through the bouncing paths, or undergo diffusive motion, for long time. One may argue that the particle motion occurs in a system of size L, in which it has a diffusive path and hence the average escape time $t_c \sim L^2/D$, with D the diffusion coefficient. Thus the escape rate $\gamma \sim D/L^2$. A more general expression for diffusion coefficient D is derived through the escape rate formula in Ref. [39]. For the Lorentz gas with large L, by taking the general form of the escape rate $\gamma = \lambda - h_{ks}$, where λ is the Lyapunov exponent and h_{KS} is the Kolmogorov-Sinai entropy of the fractal repeller $\mathcal{F}_L$, one has $D = [L/2.40482]^2 \left[\lambda(\mathcal{F}_L) - h_{KS}(\mathcal{F}_L)\right]$.

There is a fundamental connection between the present observation of classical resonances and the diffusion operator approach of the supersymmetry theories [43] of disordered systems. The statistics of the spectra and eigenfunction of disordered systems is directly related to the classical spectral determinant $D(\varepsilon) = \varepsilon^{-2} \prod_\mu (1 + \varepsilon^2\Delta^2/\gamma_\mu^2)^{-1}$, where ε is the energy (in unit of Δ, the average level spacing), and γ_μ are the non-zero eigenvalues of the diffusion operator [44, 45]. These are just the RP resonances that we have observed in open systems. Using the supersymmetric techniques, Agam, Altshuler, and Andreev [46] calculated the level correlation and showed that it can be fully determined by the classical spectrum of the Perron-Frobenius operator. Bogomolny and Keating [47] arrived at a similar conclusion using the periodic orbit approach. The applicability of these theories for closed systems is currently a matter of debate [48], but the applicability of the supersymmetry theory to disordered systems is well established, and is strongly supported by microwave experiments on disordered billiards [23, 42].

As pointed out by Berry [4], the two limits $T \to \infty$ and $\hbar \to 0$ do not commute with each other, thus the long-time quantum evolution is fundamentally different from long time classical evolution. The probability P_q that the quantum chaotic system decays at time t after its formation follows a power law [49, 24] $P_q(t) \sim (1+2\overline{\Gamma}t)^{-2-\frac{M}{2}}$, for t larger than the equilibrium time of the system. Here $\overline{\Gamma}$ is the average decay width, M the number of open channels. As the system is opened up with more channels, the decay will be almost exponential since the above equation can be approximated by $P_q(t) \sim \exp\left[-(4+M)\overline{\Gamma}t\right]$, for large M and the weight of the algebraic tail becomes negligible. More precisely, as pointed out in Ref. [50], there exists a new quantum relaxation time scale $t_q < t_H$, with $t_H = \hbar/\Delta$ the Heisenberg time. Beyond that time, the quantum correlation decays algebraically. For shorter times, the quantum correlation decays exponentially in the same way as the classical correlation does. For an open system, since the spectrum is continuous, the Heisenberg time is actually infinite, and so is the quantum relaxation time t_q. This is one reason that the classical resonances are clearly visible in the present experiments, and the Lorentzian decomposition of the spectral autocorrelation works so well.

The transmission spectrum measured in the microwave experiment directly corresponds to the conductivity measured in electronic quantum dots. In quantum dot experiments though, the magnetoconductivity $\sigma(B)$ is typically measured, so that the resulting autocorrelation $C(\Delta B)$ is related to the area spectrum, rather than the wave vector dependence $C(\kappa)$ measured here which is related to the length spectrum [34]. Nevertheless similar arguments should be applicable there also, as well as to a variety of other physical systems which are essentially open and chaotic, such as molecular photo-dissociation [51] and chemical reactions [5].

While the coupling to the quantum resonances is well understood, the statistics and also the physical meaning of the experimental coupling b_n to the classical resonances in Eq. (4) deserves further clarification. It would also be very interesting to examine the role of classical resonances in mixed phase space systems [52], such as the open billiards frequently considered in quantum dots where the classical decay is non-exponential [53]. More detailed work should be devoted to these and other interesting questions raised by the present results.

Acknowledgements

We have benefited greatly from formal and informal discussions at the “Quantum Chaos Y2K” Nobel Symposium. We thank P. Cvitanović and O. Agam for important insights into the semiclassical arguments for the correspondence between quantum and classical correlations. We also thank O. Bohigas, B. Altshuler, J. Keating, E. Bogomolny, D. Ullmo and P. Lebeouf for useful discussions.

This work was supported by NSF-PHY-9722681.

References

[1] Gutzwiller, M. C., “Chaos in Classical and Quantum Mechanics”, (Springer, New York, 1990).

[2] Bohigas, O., “Chaos and Quantum Physics”. (Edited by Giannoni, M.-J., Voros, A., and Zinn-Justin, J.) (Elsevier Science Publishers, 1991), p.87 and references therein.

[3] Guhr, T., Müller-Groeling , A. and Weidenmüller, H. A., Phys. Rep. **299**, 189 (1998) and references therein.

[4] Berry, M., “Chaos and Quantum Physics”. (Edited by Giannoni, M. -J., Voros, A., and Zinn-Justin, J.) (Elsevier Science Publishers, 1991), p251.

[5] Gaspard, P. and Rice, S. A., J. Chem. Phys. **90**, 2225 (1989); **90**, 2242 (1989); **90**, 2255 (1989); **91**, E3279 (1989).

[6] Kadanoff, L. P. and Tang, C., Proc. Natl. Acad. Sci. USA **81**, 1276 (1984).

[7] Ruelle, D., Phys. Rev. Lett. **56**, 405 (1986); J. Stat. Phys. **44**, 281 (1986).

[8] Pollicott, M., Inv. Math. **81**, 413 (1985); *ibid.* **85**, 147 (1986); Ann. Math. **131**, 331 (1990).

[9] Gaspard, P. and Alonso Ramirez, D., Phys. Rev. A **45**, 8383 (1992); Gaspard, P., "Chaos, Scattering and Statistical Mechanics", (Cambridge University press, Cambridge, 1998).

[10] Cvitanović, P. and Eckhardt, B., Nonlinearity **6**, 277 (1993); Cvitanović, P., Artuso, R., Mainieri, R., and Vattay, G., "Classical and Quantum Chaos: a Cyclist Treatise", http://www.nbi.dk/ChaosBook/.

[11] Gaspard, P., Alonso, D., Okuda, T. and Nakamura, K., Phys. Rev. E **50**, 2591 (1994).

[12] Lu, W., Rose, M., Pance, K. and Sridhar, S., Phys. Rev. Lett. **82**, 5233 (1999).

[13] Lu, W., Viola, L., Pance, K., Rose, M. and Sridhar, S., Phys. Rev. E **61**, 3652 (2000); *ibid.* **62**, 4478 (2000) and reference therein.

[14] As discussed in subsequent sections, the POs underly the description of both the quantum and classical resonances.

[15] Pance, K., Lu, W. and Sridhar, S., Phy. Rev. Lett. **85**, 2737 (2000).

[16] Datta, S., "Electronic Transport in Mesoscopic Systems", (Cambridge University Press, Cambridge, 1995).

[17] Cvitanović, P. and Eckhardt, B., Phys. Rev. Lett. **63**, 823 (1989).

[18] Cvitanović, P., Rosenqvist, P. E. and Vattay, G., Chaos **3**, 619 (1993).

[19] Main, J., Phys. Rep. **316**, 233 (1999).

[20] Wirzba, A., Chaos **2**, 77 (1992).

[21] Cvitanović, P. and Eckhardt, B., J. Phys. A **24**, L237 (1991).

[22] Ruelle, D., "Thermodynamics Formalism", Encyclopedia of Mathematics, Vol. 5 (Addison-Wesley, Reading, MA, 1978).

[23] Kudrolli, A., Kidambi, V., and Sridhar, S., Phys. Rev. Lett. **75**, 822 (1995).

[24] Alt, H. *et al*, Phys. Rev. Lett. **74**, 62 (1995).

[25] Stein, J., Stöckmann, H.-J. and Stoffregen, U., Phys. Rev. Lett. **75**, 53 (1995).

[26] Stöckmann, H.-J., "Quantum chaos: an introduction", (Cambridge University Press, Cambridge, 1999).

[27] Jackson, J. D., "Classical Electrodymanics", second edition, (John Wiley & Sons, Inc., 1975).

[28] Fyodorov, Y. V., Titov, M. and Sommers, H. -J., Phys. Rev. E **58**, R1195 (1998); Fyodorov, Y. Y. and Khoruzhenko, B. A., Phys. Rev. Lett. **83**, 65 (1999), Fyodorov, Y. V. and Sommers, H. -J., J. Math. Phys. **38**, 1918 (1997).

[29] Cvitanović, P., private communication.

[30] Eckhardt, B., Chaos **3**, 613 (1993).

[31] Christiansen, F., Paladin, G. and Rugh, H. H., Phys. Rev. Lett. **65**, 2087 (1990).

[32] Agam, O., Phys. Rev. E **61**, 1285 (2000).

[33] Blümel, R. and Smilansky, U., Phys. Rev. Lett. **60**, 477 (1988).

[34] Jalabert, R. A., Baranger, H. U. and Stone, A. D., Phys. Rev. Lett. **65**, 2442 (1990).

[35] Lewenkopf, C. H. and Weidenmüller, H. A., Ann. Phys. **212**, 53 (1991).

[36] Lai, Y.-C., Blümel, R., Ott, E. and Grebogi, C., Phys. Rev. Lett. **68**, 3491 (1992).

[37] Biswas, D. and Sinha, S., Phys. Rev. Lett. **71**, 3790 (1993).

[38] Bohigas, O., (unpublished).

[39] Gaspard, P. and Niclois, G., Phys. Rev. Lett. **65**, 1693 (1990).

[40] Hasegawa, H. H. and Saphir, W. C., Phys. Rev. A **46**, 7401 (1992).

[41] Dorfman, J. R., "An introduction to chaos in nonequilibrium statistical mechanics", (Cambridge University Press, Cambridge, 1999).

[42] Pradhan, P. and Sridhar, S., Phys. Rev. Lett. **85**, 2360 (2000).

[43] Efetov, K. B., Adv. Phys. **32**, 53(1983); Efetov, K. B., "Supersymmetry in Disorder and Chaos", (Cambridge University Press, Cambridge, 1997).

[44] Andreev, A. V. and Altshuler, B. L., Phys. Rev. Lett. **75**, 902 (1995).

[45] Mirlin, A. D., Phys. Rep. **326**, 259 (2000).

[46] Agam, O., Atshuler, B. L. and Andreev, A. V., Phys. Rev. Lett. **75**, 4389 (1995).

[47] Bogomolny, E. B. and Keating, J. P., Phys. Rev. Lett. **77**, 1472 (1996).

[48] Prange, R. E., Phys. Rev. Lett. **78**, 2280 (1997).

[49] Harney, H. L., Dittes, F.-M., and Müller, A., Ann. Phys. (N.Y.) **220**, 159 (1992).

[50] Casati, G., Maspero, G., and Shepelyansky, D. L., Phys. Rev. E **56**, R6233 (1997); Savin, D. V. and Sokolov, V. V., *ibid.* **56**, R4911 (1997); Fraham, K. M., *ibid.* **56**, R6237 (1997).

[51] Agam, O., Phys. Rev. A **60**, R2633 (1999).

[52] Weber, J., Haake, F. and Seba, P., Phys. Rev. Lett. **85**, 3620 (2000).

[53] Ketzmerick, R., Phys. Rev. B **54**, 10841 (1996).

Table 1: Experimental and theoretical RP resonances of the 4-disk system in the fundamental domain with $R/a = 4\sqrt{2}$ and $a = 5$ cm. The RP resonances are in the unit of cm^{-1}.

γ''_{exp}	γ''_{th}	γ'_{exp}	γ'_{th}
0.000	0.000	0.049	0.0599
0.187	0.242	0.053	0.0980
0.378	0.386	0.051	0.0910
0.515	0.468	0.165	0.1682
0.632	0.629	0.079	0.0647
0.842	0.868	0.055	0.0841
1.016	1.027	0.045	0.0785
1.060	1.125	0.096	0.1067
1.254	1.255	0.060	0.0718

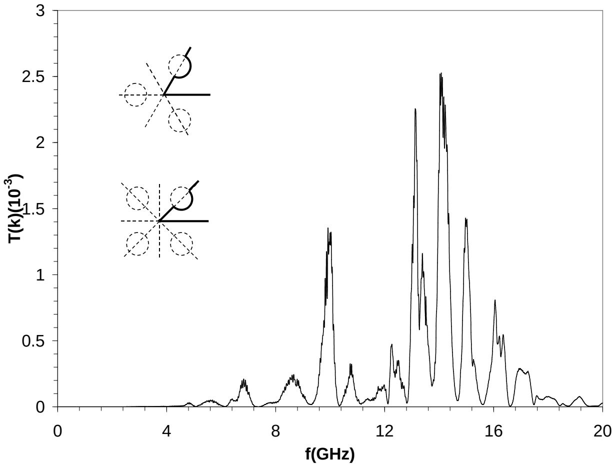

Figure 1: Experimental transmission $T(k)$ of the 4-disk system in the fundamental domain with $R/a = 4\sqrt{2}$ and $a = 5$ cm. Here $f = (c/2\pi)k$. Inset: Geometry of the 3- and 4-disk billard. The solid lines represent the fundamental domain in which the experiments were carried out.

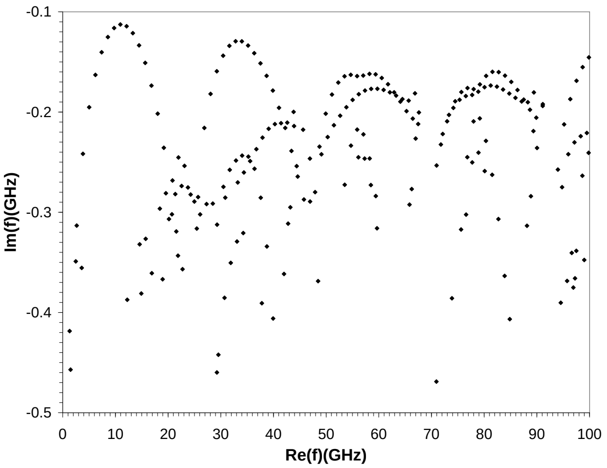

Figure 2: Quantum resonances in the A_2 representation of the 3-disk system with $R/a = 4\sqrt{3}$ with $a = 5$ cm in the fundamental domain. The quantum resonances we observed experimentally are in the range $0 < f < 20GHz$. See [13] for details.

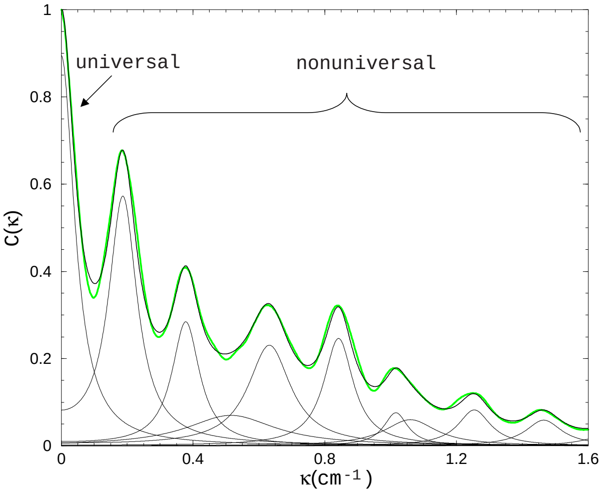

Figure 3: Autocorrelation function $C(\kappa)$ vs κ (cm^{-1}) of the 4-disk system in the fundamental domain with $R/a = 4\sqrt{2}$ and $a = 5$ cm. The gray line is the experimental $C(\kappa)$ calculated from the experimental trace shown in Fig. 1. The data show the small κ universal behavior followed by the non-universal oscillations for large κ. The entire autocorrelation $C(\kappa)$ can be described in terms of the RP resonances using Eq.(4) (thick solid line). The thin lines represent the Lorentzian decomposition into individual RP resonances.

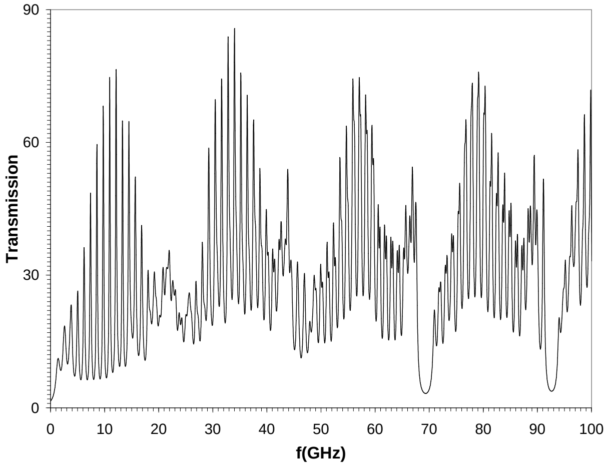

Figure 4: Numerical spectral transmission $\overline{T(k)}$ in the fundamental domain of the 3-disk system for $R/a = 4\sqrt{3}$ and $a = 5$ cm.

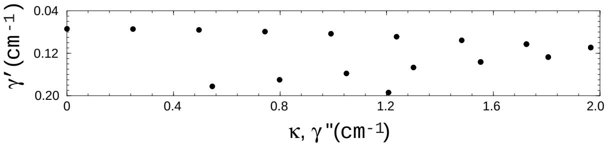

Figure 5: Numerical spectral autocorrelation $C(\kappa)$ (top) and RP resonances $\gamma' \pm i\gamma''$ (bottom) for the 3-disk system with $R/a = 4\sqrt{3}$ and $a = 5$cm in the fundamental domain. $C(\kappa)$ was calculated from the numerical spectrum shown in Fig. 4 for interval $\Delta k = 6\text{cm}^{-1}$ with the central values k_0 in cm^{-1} indicated in the figure.